Breaking the exponential wall in classical simulations of fidelity

Cesare Mollica, Tomáš Zimmermann, and Jiří Vaníček*
Laboratory of Theoretical Physical Chemistry, Institut des Sciences et Ingénierie Chimiques, Ecole Polytechnique Fédérale de Lausanne, Lausanne, Switzerland
(Dated: August 2, 2011)

We analyze the efficiency of available algorithms for the simulation of classical fidelity and show that their computational costs increase exponentially with the number of degrees of freedom for almost all initial states. Then we present an algorithm whose cost is independent of the system's dimensionality and show that, within a continuous family of algorithms, our algorithm is the only one with this property. Simultaneously we propose a general analytical approach to estimate efficiency of trajectory-based methods.

PACS numbers: 05.45.-a, 05.45.Jn, 05.45.Mt, 05.45.Pq

Introduction. While the solution of the time-dependent Schrödinger equation scales exponentially with dimensionality and is feasible for only a few continuous degrees of freedom (DOF), classical (CL) molecular dynamics simulations are, in principle, feasible for millions of atoms. It may therefore be surprising that papers studying classical fidelity (CF) have provided numerical results for only one or a few DOF [1–4]. A notable exception is Ref. [5], which, for the largest systems, relies on initial densities given by characteristic functions. Below we explain this situation by showing that not only quantum (QM) but also all previously used CL algorithms for fidelity scale exponentially with the number D of DOF for initial states other than characteristic functions. Hence even when QM effects are negligible and CL picture is appropriate, the "simple" CL simulations may be unfeasible. Since numerical simulations are important for testing analytical theories of CF in large systems, we design an efficient CF algorithm that avoids the exponential scaling with D.

Quantum and classical fidelity. While important in its own right, CF can be viewed as the CL limit of quantum fidelity (QF) [6], introduced by Peres [7] to measure the stability of QM dynamics (QD). QF is the squared overlap $F_{\text{QM}}(t)$ at time t of two quantum states, identical at $t = 0$, but evolved with two different Hamiltonians, H_0 and $H_\epsilon = H_0 + \epsilon V$:

$$F_{\text{QM}}(t) := |f_{\text{QM}}(t)|^2, \tag{1}$$

$$f_{\text{QM}}(t) := \langle\psi\,|U_\epsilon^{-t}U_0^t|\,\psi\rangle, \tag{2}$$

where $f_{\text{QM}}(t)$ is the fidelity amplitude and $U_\epsilon^t := \exp(-iH_\epsilon t/\hbar)$ the QM evolution operator. Rewriting Eq. (2) as $f_{\text{QM}}(t) = \langle\psi\,|U^t|\,\psi\rangle$ with the echo operator $U^t := U_\epsilon^{-t}U_0^t$, it can be interpreted as the Loschmidt echo, i.e., an overlap of an initial state with a state evolved for time t with H_0 and subsequently for time $-t$ with H_ϵ. (In general, we write time t as a superscript. Subscript ϵ denotes that H_ϵ was used for dynamics. If an evolution operator, phase space coordinate, or density lacks a subscript, Loschmidt echo dynamics is implied.) QF amplitude (2) is ubiquitous in applications: it appears in NMR spin echo experiments [8], neutron scattering [9], ultrafast electronic spectroscopy [10], etc. QF (1) is relevant in QM computation and decoherence [11], and can be used to measure nonadiabaticity [12] or accuracy of molecular QD on an approximate potential energy surface [13].

Definition (1) can be generalized to mixed states in different ways [6, 14], but we will assume that the initial states are pure. In this case, one may always write QF (1) as $F_{\text{QM}}(t) = \text{Tr}\,(\hat\rho_\epsilon^t\hat\rho_0^t)$ where $\hat\rho_\epsilon^t := U_\epsilon^t\hat\rho U_\epsilon^{-t}$ is the density operator at time t. In the phase-space formulation of QM mechanics, QF becomes $F_{\text{QM}}(t) = h^{-D}\int dx\rho_{\epsilon,\text{W}}^t(x)\rho_{0,\text{W}}^t(x)$ where $x := (q,p)$ is a point in phase space and $A_\text{W}(x) := \int d\xi\langle q-\xi/2\,|A|\,q+\xi/2\rangle e^{ip\xi/\hbar}$ is the Wigner transform of A. This alternative form of QF provides a direct connection to its CL limit, which is precisely the CF, defined as [1, 2]

$$F_{\text{CL}}(t) := F_{\text{fid}}(t) = h^{-D}\int dx\rho_\epsilon^t(x)\rho_0^t(x) \tag{3}$$

$$= F_{\text{echo}}(t) = h^{-D}\int dx\rho^t(x)\rho^0(x) \tag{4}$$

where the first and second line express CF in the fidelity and Loschmidt echo pictures, respectively, ρ_ϵ^t is the CL phase-space density evolved with H_ϵ, and ρ^t is this density evolved under the echo dynamics. We omit subscript "CL" for CL quantities F and ρ since CF is the main subject of this paper.

Algorithms. The exponential scaling of QD with D is well known. As for CF, Eqs. (3)-(4) may be evaluated, e.g., with trajectory, grid, or mesh-based methods. Clearly, the grid-based methods would suffer from a similar exponential scaling as QD on a grid. We focus on the most general and straightforward trajectory-based methods, which are obtained from Eqs. (3)-(4) using the Liouville theorem, yielding equivalent expressions

$$F_{\text{fid}}(t) = h^{-D}\int dx^0\rho(x_\epsilon^{-t})\rho(x_0^{-t}) \text{ and} \tag{5}$$

$$F_{\text{echo}}(t) = h^{-D}\int dx^0\rho(x^{-t})\rho(x^0). \tag{6}$$

Above, $x_\epsilon^t := \Phi_\epsilon^t(x^0)$ where Φ_ϵ^t is the Hamiltonian flow of H_ϵ and $x^t := \Phi^t(x^0)$ where $\Phi^t := \Phi_\epsilon^{-t}\circ\Phi_0^t$ is the Loschmidt echo flow. Since it is the phase space points rather than the densities that evolve in expressions (5)-(6), we can take $\rho = \rho_\text{W}$, i.e., the Wigner transform of the initial QM state. We further rewrite Eqs. (5)-(6) in a form suitable for Monte Carlo evaluation, i.e., as an average

$$\big\langle A(x^0,t)\big\rangle_{W(x^0)} := \frac{\int dx^0 A(x^0,t)W(x^0)}{\int dx^0 W(x^0)}$$

where W is the sampling weight for initial conditions x^0. The weight can be any positive definite function, but it is advantageous to consider the weight to be related to the density ρ. While previously used algorithms sampled from ρ [2, 4, 5], we consider more general weights $W = W_M(x^0) := \rho(x^0)^M$ and $W = W_M(x_0^{-t}) = \rho(\Phi_0^{-t}(x^0))^M$ for the echo and fidelity dynamics, respectively. These weights yield M-dependent algorithms

$$F_{\text{fid-}M}(t) = I_M \langle \rho(x_\epsilon^{-t})\rho(x_0^{-t})^{1-M} \rangle_{\rho(x_0^{-t})^M}, \quad (7)$$

$$F_{\text{echo-}M}(t) = I_M \langle \rho(x^{-t})\rho(x^0)^{1-M} \rangle_{\rho(x^0)^M}, \quad (8)$$

where $I_M := h^{-D} \int \rho(x^0)^M dx^0$ is a normalization factor. In both families of algorithms (7)-(8), sampling can be done by Metropolis Monte Carlo for general dynamics and any positive definite weight ρ^M. For $M > 0$, the echo algorithms (8) are, however, much more practical since the initial state is often known explicitly (and generally is much smoother than the final state), making sampling easier. Furthermore, for simple initial states such as Gaussian wavepackets (GWPs), the Metropolis sampling in the echo algorithms can be replaced by analytical sampling. Therefore, for $M > 0$ the fidelity algorithms are more of a theoretical possibility than a practical tool. For $M = 0$, the sampling is uniform and makes sense only for a compact phase space of finite volume $\Omega = \Omega_1^D = (n_1 h)^D$ where Ω_1 and n_1 are respectively the phase space volume and Hilbert-space dimension for a single DOF. For $M > 0$, importance sampling based on the weight W_M is used and an infinite phase space is allowed. For general M, the sampling is only defined for CL states (such as GWPs), for which $\rho \geq 0$. However, for $M = 0$ and for the important special case of $M = 2$, the sampling is defined for any pure state, i.e., even for negative values of ρ.

In order to compute CF directly from algorithms (7) or (8), the normalization factor I_M must be known analytically. For general pure states, I_M is known analytically only for $M = 0, 1,$ or 2. For $M = 0$, $I_0 = n_1^D$ because of the requirement of finite phase space. For both $M = 1$ and $M = 2$, $I_M = 1$ since $\mathrm{Tr}\,\hat{\rho} = \mathrm{Tr}\,\hat{\rho}^2 = 1$. For $M \notin \{0, 1, 2\}$, algorithms (7) and (8) can only be used for special initial states. E.g., for initial GWPs $\rho(x) = g(x; X, a) := 2^D \exp\left[-(q-Q)^2/a^2 - (p-P)^2 a^2/\hbar^2\right]$ where X is the center and a the width of the GWP, we have $I_M = \left(2^{M-1}/M\right)^D$ for general $M > 0$. However, the unknown normalization factor can be removed from Eqs. (7) and (8) by dividing them by the value of I_2 [note that $I_2(0) = F(0)$] obtained with the same algorithm and trajectories. Resulting "normalized" (N) algorithms,

$$F_{\text{fid-N-}M}(t) := \frac{F_{\text{fid-}M}(t)}{I_2(t)} = \frac{\langle \rho(x_\epsilon^{-t})\rho(x_0^{-t})^{1-M} \rangle_{\rho(x_0^{-t})^M}}{\langle \rho(x_0^{-t})^{2-M} \rangle_{\rho(x_0^{-t})^M}}, \quad (9)$$

$$F_{\text{echo-N-}M}(t) := \frac{F_{\text{echo-}M}(t)}{I_2(0)} = \frac{\langle \rho(x^{-t})\rho(x^0)^{1-M} \rangle_{\rho(x^0)^M}}{\langle \rho(x^0)^{2-M} \rangle_{\rho(x^0)^M}}, \quad (10)$$

are practical for general initial states and for any M. As far as we know, from the four families of algorithms (7), (8), (9), and (10) only echo-1 (8) has been used previously [2, 4, 5]. Note however, that for initial states given by characteristic functions, echo-1 = echo-M = echo-N-M for all $M > 0$.

Efficiency. The cost of a typical method propagating N trajectories for time t is $O(c_{\text{f}} t N)$ where c_{f} is the cost of a single force evaluation. However, among the above mentioned algorithms, this is only true for the fidelity algorithms with $M = 0$. Remarkably, in all other cases, the cost is $O(c_{\text{f}} t^2 N)$. For a single time t, the cost is linear in time, but if one wants to know CF for all times up to t, the cost is quadratic with t. For the echo algorithms, it is because one must make full backward propagation for each time between 0 and t. For the fidelity algorithms, it is because the weight function $\rho(x^{-t})^M$ changes with time and the sampling has to be redone from scratch for each time between 0 and t. In other words, different trajectories are used for each time between 0 and t.

The above estimates are correct but not the full story. There are hidden costs since the number of trajectories N required for convergence can depend on D, t, dynamics, initial state, and method. One usually empirically increases N until convergence, but this is often impracticable. Instead, we estimate N analytically. An essential point is that N is fully determined by the desired discretization error σ_{discr}. The expected systematic component of σ_{discr} is zero or $O(N^{-1})$ for all cases studied and is negligible to the expected statistical component $\sigma = O(N^{-1/2})$ which therefore determines convergence. This statistical error is computed as $\sigma^2(t, N) = \overline{F(t,N)^2} - \overline{F(t,N)}^2$ where the overline denotes an average over infinitely many independent simulations with N trajectories. Hence we can formulate the problem of efficiency precisely: "What N is required to converge fidelity F to within a statistical error σ?" We let N be a function of F because in many applications, one is interested in F above a certain threshold value F_{min}. This threshold can vary with application: it may be close to unity (in quantum computing) or to zero (yet finite, in calculations of spectra), but in general will be *independent* of D.

The discretized form of Eq. (7) is $F_{\text{fid-}M}(t, N) = I_M N^{-1} \sum_{j=1}^N \rho_{\text{CL}}(x_{\epsilon,j}^{-t}) \rho_{\text{CL}}(x_{0,j}^{-t})^{1-M}$, from which $\overline{F_{\text{fid-}M}(t,N)^2} = I_M^2 N^{-1} \langle \rho(x_\epsilon^{-t})^2 \rho(x_0^{-t})^{2-2M} \rangle_{\rho(x_0^{-t})^M} + (1 - N^{-1}) F^2$. Similarly, from Eq. (8) $\overline{F_{\text{echo-}M}(t,N)} = I_M N^{-1} \sum_{j=1}^N \rho(x_j^{-t}) \rho(x_j^0)^{1-M}$, hence $\overline{F_{\text{echo-}M}(t,N)^2} = I_M^2 N^{-1} \langle \rho(x^{-t})^2 \rho(x^0)^{2-2M} \rangle_{\rho(x^0)^M} + (1 - N^{-1}) F^2$.

Realizing that $\overline{F_{\text{fid-}M}(t,N)} = \overline{F_{\text{echo-}M}(t,N)} = F(t)$ in both cases, we obtain the same error

$$\sigma_{\text{fid-}M}^2 = \sigma_{\text{echo-}M}^2 = N^{-1}(I_M J_M - F^2), \quad (11)$$

$$J_M := h^{-D} \int dx^0 \rho(x^{-t})^2 \rho(x^0)^{2-M}. \quad (12)$$

In the special case of $M = 2$, we find our *main result*,

$$\sigma_{\text{fid-2}}^2 = \sigma_{\text{echo-2}}^2 = N^{-1}\left(1 - F^2\right). \quad (13)$$

This expression shows that for general states and for general dynamics, statistical error of $F_{\text{fid-2}}$ or of $F_{\text{echo-2}}$ depends only on N and F. In other words, the number of trajectories needed for convergence is *independent* of t, D, or dynamics of the system. This important result is due to the fact that for the sampling weight $W = \rho^2$, each numerical trajectory contributes evenly to the weighted average (at time $t = 0$).

As for algorithms (7)-(8) with $M \neq 2$, one might hope to improve convergence by employing the normalized versions (9)-(10). The error analysis is simplified using the formula for statistical error of a ratio of two random variables,

$$\left(\frac{\sigma_{A/B}}{\overline{A/B}}\right)^2 = \left(\frac{\sigma_A}{\bar{A}}\right)^2 + \left(\frac{\sigma_B}{\bar{B}}\right)^2 - 2\frac{\overline{AB} - \bar{A}\bar{B}}{\bar{A}\bar{B}}. \quad (14)$$

In our case, $F_{\text{N-}M}(t,N) = A/B$ where $A = F_M(t,N)$, $B = F_M(0,N)$, $\bar{A} = F(t)$, $\bar{B} = F(0) = 1$, and σ_A and σ_B are given by Eq. (11). The only unknown in Eq. (14) is $\overline{AB}$. For the normalized echo algorithms (10), we have $\overline{AB} = \overline{F_{\text{echo-}M}(t,N)F_{\text{echo-}M}(0,N)} = I_M^2 N^{-1}\langle\rho(x^{-t})\rho(x^0)^{3-2M}\rangle_{\rho(x^0)^M} + (1-N^{-1})F(t)F(0) = N^{-1}I_M K_M + (1-N^{-1})F$ where $K_M := h^{-D}\int dx^0\,\rho(x^{-t})\rho(x^0)^{3-M}$. The same derivation goes through for the fidelity algorithms. The final error can in both cases be written as

$$\sigma^2_{\text{N-}M} = N^{-1}\left(J_M - 2K_M F + I_{4-M}F^2\right). \quad (15)$$

Exponential growth of the error for $M \neq 2$. Now we will show that the special case $M = 2$ is unique and that all the other above-mentioned algorithms (which include all the algorithms available in the literature) have an error growing exponentially with D. Since we are searching for counterexamples, special cases are sufficient. For us these will be initial GWP states and "pure displacement" (PD) or "pure squeezing" (PS) dynamics [3]. All calculations can be done analytically using special cases of the integral

$$\int dq \exp[-c_1(q-q_1)^2 - c_2(q-q_2)^2]$$
$$= \left(\frac{\pi}{c_1+c_2}\right)^{D/2} \exp\left[-\frac{c_1 c_2}{c_1+c_2}(q_1-q_2)^2\right].$$

In the PD case, the center of the GWP moves while both its shape and size remain constant. Such fidelity dynamics can be realized exactly by two displaced simple harmonic oscillator (SHO) potentials with equal force constants. For PD, the width $a_0^t = a_\epsilon^t = a^t = a^0 = a$ and either $X_\epsilon^t = X_0^t + \Delta X^t$ or $X^t = X^0 + \Delta X^t$. CF is $F(t) = h^{-D}\int dx\, g(x;X^t,a)g(x;X^0,a) = \exp\left\{-\frac{1}{2}\left[\left(\frac{\Delta Q^t}{a}\right)^2 + \left(\frac{\Delta P^t a}{\hbar}\right)^2\right]\right\}$ and the factor (12) needed in the statistical error can be expressed in terms of F as $J_M = \left(\frac{2^{3-M}}{4-M}\right)^D F^{\gamma_M}$ with $\gamma_M = 4 - 8/(4-M)$. Using this result in Eq. (11), the statistical errors are

$$\sigma^2_{\text{fid-}M,\,\text{PD}} = \sigma^2_{\text{echo-}M,\,\text{PD}} = \frac{1}{N}\left(\beta_M^D F^{\gamma_M} - F^2\right), \quad (16)$$

$$\beta_0 = 2n_1 \text{ and } \beta_{0<M<4} = \frac{4}{(4-M)M}. \quad (17)$$

Note that $\beta_M \geq 1$ and the minimum $\beta_2 = 1$ is achieved for $M = 2$. The minimum agrees precisely with the general result (13). Except for $M = 2$, $\beta_M > 1$, showing that even in the simple case of PD dynamics, the errors of all algorithms from the families (7) and (8) grow *exponentially* with D, which is the *second major result* of this paper. The normalized methods (9) and (10) lower the prefactor of the error but do not change the exponential scaling with D: Since $K_M = [2^{3-M}/(4-M)]^D F^{\delta_M - 1}$ where $\delta_M = 3 - 2/(4-M)$, statistical errors are

$$\sigma^2_{\text{fid-N-}M,\,\text{PD}} = \sigma^2_{\text{echo-N-}M,\,\text{PD}} = N^{-1}\beta_M^D\left(F^{\gamma_M} + F^2 - 2F^{\delta_M}\right).$$

In the PS case, the center of the GWP remains fixed while its width narrows in some directions and spreads in others. Such fidelity dynamics is realized exactly by two inverted SHOs with common centers and different force constants. Analytical calculations show that the errors of different algorithms again grow *exponentially* with D (see Table I).

To summarize, in all cases studied, for $D \gg 1$ the number of trajectories required for a specified convergence is

$$N = \sigma^{-2}\alpha(F)\beta^D \quad (18)$$

where α and β depend on the method and dynamics and are listed in Table I. For both fidelity and echo algorithms with $M = 2$, for any dynamics and any initial state, the coefficient $\beta = 1$, implying independence of D. Note also that algorithms with $M = 2$ are automatically normalized. For all other algorithms (both echo and fidelity, both unnormalized and normalized, and for any $M \neq 2$) and for both PD and PS dynamics, $\beta > 1$, implying an exponential growth with D. This growth is dramatic for $M = 0$ ($\beta = 2n_1 \gg 1$): since n_1^D is the Hilbert space dimension, the cost of $M = 0$ algorithms approaches that of QF. This is unfortunate since $F_{\text{fid-0}}$ is the only algorithm that scales linearly in time. On the other hand, for the most intuitive and most common $M = 1$ algorithms, $\beta = 4/3$ or $\sqrt{2}$, and the growth is much slower, although still exponential. We cannot exclude existence of a faster CL algorithm; however, we doubt existence of a CL algorithm that would be *both* linear in t *and* independent of D.

*Numerical results and conclusion.*To illustrate the analytical results obtained above, numerical tests were performed in multidimensional systems of uncoupled displaced SHOs (for PD dynamics), inverted SHOs (for PS dynamics), and perturbed kicked rotators (for nonlinear integrable and chaotic dynamics). The last model is defined, $\text{mod}(2\pi)$, by the map $q_{j+1} = q_j + p_j$, $p_{j+1} = p_j - \nabla W(q_{j+1}) - \epsilon\nabla V(q_{j+1})$ where $W(q) = -k\cos q$ is the potential and $V(q) = -\cos(2q)$ the perturbation of the system; k and ϵ determine the type of dynamics and perturbation strength, respectively. Uncoupled

Method	Dynamics type	$\alpha(F)$	β
fid-0	displacement	F^2	$2n_1$
fid-0	squeezing	F	$2n_1$
echo-1	displacement	$F^{4/3}$	$4/3$
echo-1	squeezing, $F \approx 1$	1	$4/3$
echo-1	squeezing, $F \ll 1$	F	$\sqrt{2}$
echo-1'	displacement	$1 - F^{4/3}$	$4/3$
echo-1'	squeezing, $F \approx 1$	$\frac{8}{9}(1-F)$	$4/3$
echo-1'	squeezing, $F \ll \left(\frac{8}{9}\right)^{\frac{D}{2}}$	1	$4/3$
echo-N-1	displacement	$F^2 + F^{4/3} - 2F^{7/3}$	$4/3$
echo-N-1	squeezing, $F \approx 1$	$\frac{8}{9}(1-F)$	$4/3$
echo-N-1	squeezing, $F \ll 1$	F	$\sqrt{2}$
echo-2	general, general state	$1 - F^2$	1

TABLE I. The number of trajectories needed to achieve a given σ is for $D \gg 1$ given by $N = \sigma^{-2}\alpha(F)\beta^D$. The table lists $\alpha(F)$ and β for different cases. Note that fid-0, echo-1, echo-1', and echo-N-1 results are for initial GWPs and exhibit exponential scaling with D while echo-2 result, valid for any initial state, is independent of D.

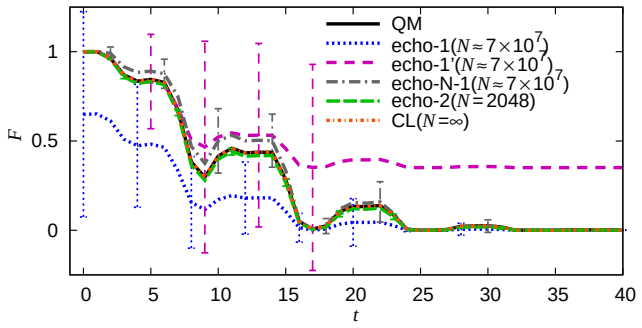

FIG. 1. Convergence of different classical fidelity algorithms in a 100-dimensional system of perturbed ($\epsilon = 10^{-4}$) quasi-integrable ($k = 0.2$) kicked rotators with $n_1 = 131072$. Algorithm echo-2 agrees with the QM result and converges with only $N = 2048$ trajectories whereas the echo-1, echo-1', and echo-N-1 results are far from converged even with $N \approx 7 \times 10^7$. Fully converged CL($N = \infty$) is computed as a product of 100 one-dimensional fidelities. The "hopelessly" unconverged fid-0 algorithm not shown. For clarity, echo-1' error bars not shown for $t > 20$.

systems were used in order to make QF calculations feasible (as a product of D 1-dimensional calculations); however, the CF calculations were performed as for a truly D-dimensional system. The initial state was always a multidimensional GWP. Expected statistical errors were estimated by averaging actual statistical errors over 100 different sets of N trajectories. No fitting was used in any of the figures, yet all numerical results agree with the analytical estimates. Note that Table I and figures show results for algorithm echo-1',

$$F_{\text{echo-1'}}(t) = 1 + \langle \rho(x^{-t}) - \rho(x^0) \rangle_{\rho(x^0)},$$

which is a variant of echo-1 accurate for high fidelity. Both echo-1 and echo-1' reduce to echo-N-1 if normalized.

Figure 1 displays fidelity in a 100-dimensional system of kicked rotators. It shows that echo-2 converges with several orders of magnitude fewer trajectories than the echo-1, echo-1', and echo-N-1 algorithms. Figures 2 and 3 confirm that $\sigma_{\text{echo-2}}$ is independent of D while $\sigma_{\text{echo-1}}$, $\sigma_{\text{echo-1'}}$, and $\sigma_{\text{echo-N-1}}$ grow exponentially with D. The normalized echo-N-1 algorithm is the most efficient among the methods with $M = 1$.

To conclude, we have shown that not only QF, but also CF algorithms can be unfeasible in complex systems due to the exponential scaling with dimensionality. We have proposed an efficient CF algorithm for which this exponential scaling disappears. In the special case of initial densities given by characteristic functions all echo-M and echo-N-M algorithms (for $M > 0$) collapse into a single algorithm. In particular, the "natural" algorithm sampling from ρ is equivalent to our algorithm sampling from ρ^2. This may explain why high-dimensional calculations were previously done only with characteristic functions. These results should be also useful in applications computing more general overlaps of phase space distributions. Finally, we have described a technique to analyze efficiency of general trajectory-based algorithms. This

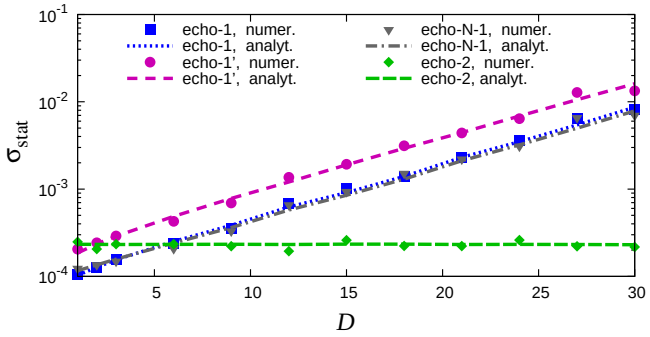

FIG. 2. Statistical error grows exponentially with D for the echo-1, echo-1', and echo-N-1 algorithms and is independent of D for the echo-2 algorithm. Dynamics corresponds to pure displacement, $N \approx 10^7$, and time was chosen separately for each D so that $F \approx 0.3$.

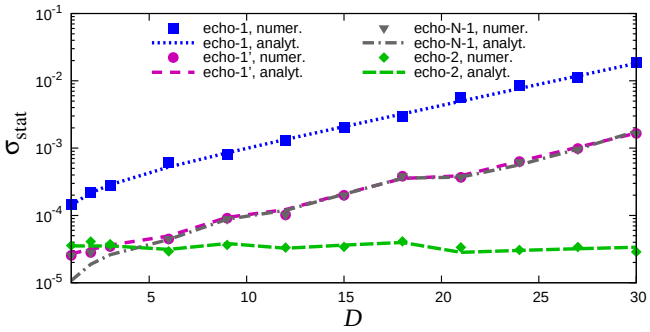

FIG. 3. Statistical error grows exponentially with D for the echo-1, echo-1', and echo-N-1 algorithms and is independent of D for the echo-2 algorithm. Dynamics corresponds to pure squeezing, $N \approx 10^7$, and time was chosen separately for each D so that $F \approx 0.99$.

can be useful in developing approximate methods for QD of large systems. Our research was supported by Swiss NSF with grants No. 200021_124936 and NCCR MUST, and by EPFL.

* jiri.vanicek@epfl.ch

[1] T. Prosen and M. Znidaric, J. Phys. A, **35**, 1455 (2002).
[2] G. Benenti and G. Casati, Phys. Rev. E, **65**, 066205 (2002).
[3] B. Eckhardt, J. Phys. A, **36**, 371 (2003); M. Combescure and A. Combescure, J. Math. Anal. Appl., **326**, 908 (2007).
[4] Z. P. Karkuszewski, C. Jarzynski, and W. H. Zurek, Phys. Rev. Lett., **89**, 170405 (2002); G. Benenti, G. Casati, and G. Veble, Phys. Rev. E, **67**, 055202 (2003); **68**, 036212 (2003); G. Veble and T. Prosen, Phys. Rev. Lett., **92**, 034101 (2004); G. Casati, T. Prosen, J. Lan, and B. Li, **94**, 114101 (2005).
[5] G. Veble and T. Prosen, Phys. Rev. E, **72**, 025202 (2005).
[6] T. Gorin, T. Prosen, T. H. Seligman, and M. Znidaric, Phys. Rep., **435**, 33 (2006); P. Jacquod and C. Petitjean, Adv. Phys., **58**, 67 (2009).
[7] A. Peres, Phys. Rev. A, **30**, 1610 (1984).
[8] H. M. Pastawski, P. R. Levstein, G. Usaj, J. Raya, and J. Hirschinger, Physica A, **283**, 166 (2000).
[9] C. Petitjean, D. V. Bevilaqua, E. J. Heller, and P. Jacquod, Phys. Rev. Lett., **98**, 164101 (2007).
[10] S. Mukamel, J. Chem. Phys., **77**, 173 (1982); Z. Li, J.-Y. Fang, and C. C. Martens, **104**, 6919 (1996); S. A. Egorov, E. Rabani, and B. J. Berne, **108**, 1407 (1998); Q. Shi and E. Geva, **122**, 064506 (2005); M. Wehrle, M. Šulc, and J. Vaníček, Chimia, **65**, 334 (2011).
[11] F. M. Cucchietti, D. A. R. Dalvit, J. P. Paz, and W. H. Zurek, Phys. Rev. Lett., **91**, 210403 (2003); T. Gorin, T. Prosen, and T. H. Seligman, New J. Phys., **6**, 20 (2004).
[12] T. Zimmermann and J. Vaníček, J. Chem. Phys., **132**, 241101 (2010); not published (2011).
[13] B. Li, C. Mollica, and J. Vaníček, J. Chem. Phys., **131**, 041101 (2009); T. Zimmermann, J. Ruppen, B. Li, and J. Vaníček, Int. J. Quant. Chem., **110**, 2426 (2010).
[14] J. Vaníček, Phys. Rev. E, **70**, 055201 (2004); **73**, 046204 (2006).